

Evaluation of Optimal Condition in Laser Shock Peening Process by AE Method

Tomoki Takata^{1,*}, Manabu Enoki¹, Akinori Matsui², Yuji Kobayashi²

¹ Department of Materials Engineering, School of Engineering, The University of Tokyo,
7-3-1 Hongo, Bunkyo-ku, Tokyo 113-8656, Japan

² Shintokogio, Ltd., 1-1-1 Nishiki, Naka-ku, Nagoya city, Aichi 460-0003, Japan

* Corresponding author's e-mail address: takata@rme.mm.t.u-tokyo.ac.jp

Abstract

Laser shock peening (LSP) is now recognized as an efficient surface treatment to improve the fatigue life of metal components. To evaluate the process conditions, Almen strip is used as well as shot peening. As this is limited to specific material and size, we cannot apply to a wide variety of substrates. Acoustic emission (AE) method is expected to be useful for understanding LSP process because an elastic wave generates when laser is radiated on a target. The water layer on a target confines the shock wave due to laser irradiations during LSP process. In this study, laser irradiations during LSP process were monitored by AE method with varying the temperature and the thickness of the water layer on a target, respectively. Impact forces during LSP process were obtained from detected AE waveforms by deconvolution technique. In addition, laser irradiations were observed by high speed camera, and the image was compared with the detected AE signal. This result shows that shock wave was emitted by not only laser ablation but also collapse of a bubble which was generated after laser irradiation and a bubble was affected by the water layer.

Keywords Laser shock peening, Acoustic emission, Cavitation bubble

1. Introduction

Peening is one of surface treatment method to improve the fatigue strength of metals by inducing compressive stresses generated from mechanical means such as hammer blows or by blasting with shot (shot peening). Laser shock peening technique, which use laser to generate the reaction force near material surface by laser ablation, can impact a layer of compressive stress four times deeper than that attainable from conventional shot peening. However, the effect of laser irradiation on materials and phenomenon near radiation point are not well understood yet. The residual stress in depth direction is generally used to evaluate the degree of laser peening. A sample for residual stress measurement has to be cut and electrochemically polished, which is a destructive method. Although there are several in-situ methods to evaluate residual stress during laser peening process such as probe beam polarization and VISAR method, these are some limitations such as an exact adjustment required for fiber position and applicability for only thin samples for the first and latter methods respectively.

Acoustic emission (AE) method is one of the nondestructive evaluation methods to evaluate the size, location and generation time of deformation and damage in real-time. AE method has been successfully applied to shot peening method to analyze impact behavior of particles and evaluate the impact force by inverse analysis [1]. In this paper, AE method was applied to laser peening process. A high speed camera was also used to observe the laser radiation behavior. The impact pressure due to laser ablation was evaluated from the detected AE signals and simulated waveforms. The laser radiation phenomenon was discussed with results of AE and high speed camera observations.

Cavitation is phenomenon that a bubble generates by pressure difference in stream and collapses with emitting shock wave after the short time. In our present group, a cavitation bubble was observed during laser shock peening process [2].

2. Experimental Procedure

2.1 Laser shock peening

Two experimental set-ups to evaluate the effects of water temperature and water thickness layer are shown in Fig. 1(a) and 1(b), respectively. A target sample was A7075 aluminum alloy with dimensions of $50 \times 50 \times 10$ mm. A Q-switched Nd:YAG laser with a wavelength of 532 nm and a pulse width of 3 – 5 ns was used for both experiments. A laser beam was focused to the center of sample using lens. The laser was irradiated at least two times for each test. In set-up of Fig. 1(a), experiment was conducted with varying laser energy and water temperature. In set-up of Fig. 1(b), experiment was conducted with varying the thickness of water layer on a target sample. The detail of experimental conditions are shown in Table 1.

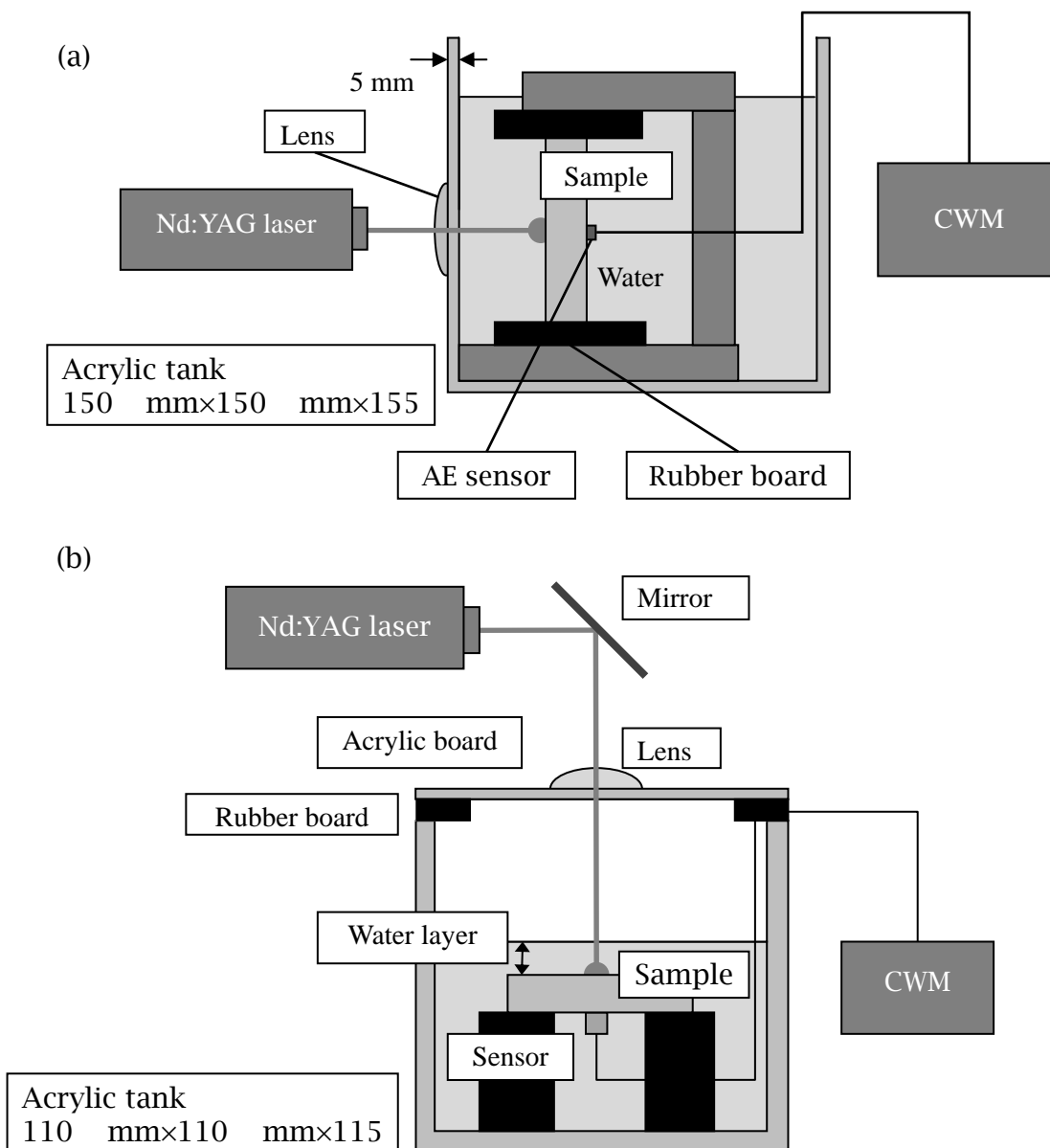


Figure 1. Schematic of experimental set-ups for studying effects of
(a) water temperature and (b) water layer thickness

Table 1. — Experimental conditions

	Laser energy	Water temperature	Water layer thickness
(a)-1	10 – 100 mJ	20 °C	-
(a)-2	100 mJ	15 - 50 °C	-
(b)	60 mJ	20 °C	1 – 10 mm

2.2 Optical observation by high speed camera

High speed cameras (Phantom Miro LC310 produced by Vision Research® Inc. and HyperVision HPV-2A produced by SHIMADZU CORPORATION) were used to observe the phenomenon during laser shock peening in experiment set-up as shown in Fig.2. The camera was set to observe the sample from an oblique direction. The phenomenon was recorded using lighting from opposite side of high speed camera. At the same time, fluctuation in water near sample surface was mainly also recorded by Phantom Miro LC310 with the sampling rate of 120,000 fps and pixels of 128×128 .

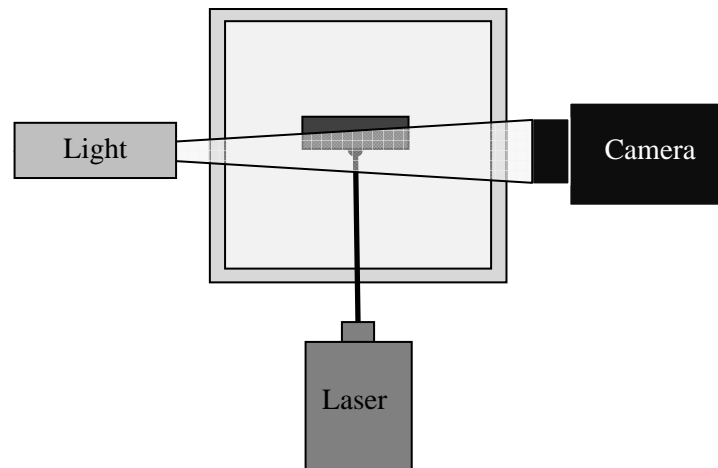


Figure 2. Top view of camera setting in Fig. 1(a)

2.3 AE measurement

An AE sensor (Pico, Physical Acoustics Corp.) was attached on the back side of the sample as shown in Fig. 1(a). Elastic waves associated with laser irradiation were recorded by Continuous Wave Memory (CWM) system, which is developed by our research group [3]. This system provides a capability to memorize all waveforms continuously at the sampling rate of 10 MHz. Waterproof paste was used to cover cables.

2.4 AE inverse analysis

Impact forces generated from laser irradiation were evaluated by an inverse analysis of AE waveform [1]. Detected AE waveform can be represented by $V(t)=S(t)*G(t)*I(t)$ where $V(t)$, $S(t)$, $G(t)$ and $I(t)$ are detected waveform, response function of sensor, Green's function of media and source function of impact force, respectively. $S(t)$ and $G(t)$ could be obtained from a simulation of AE waveform by finite element method and experimental of sharp pencil lead breaking and then $I(t)$

was estimated by the deconvolution technique. All AE waveforms were analyzed by this inverse method and obtained impact force values were discussed.

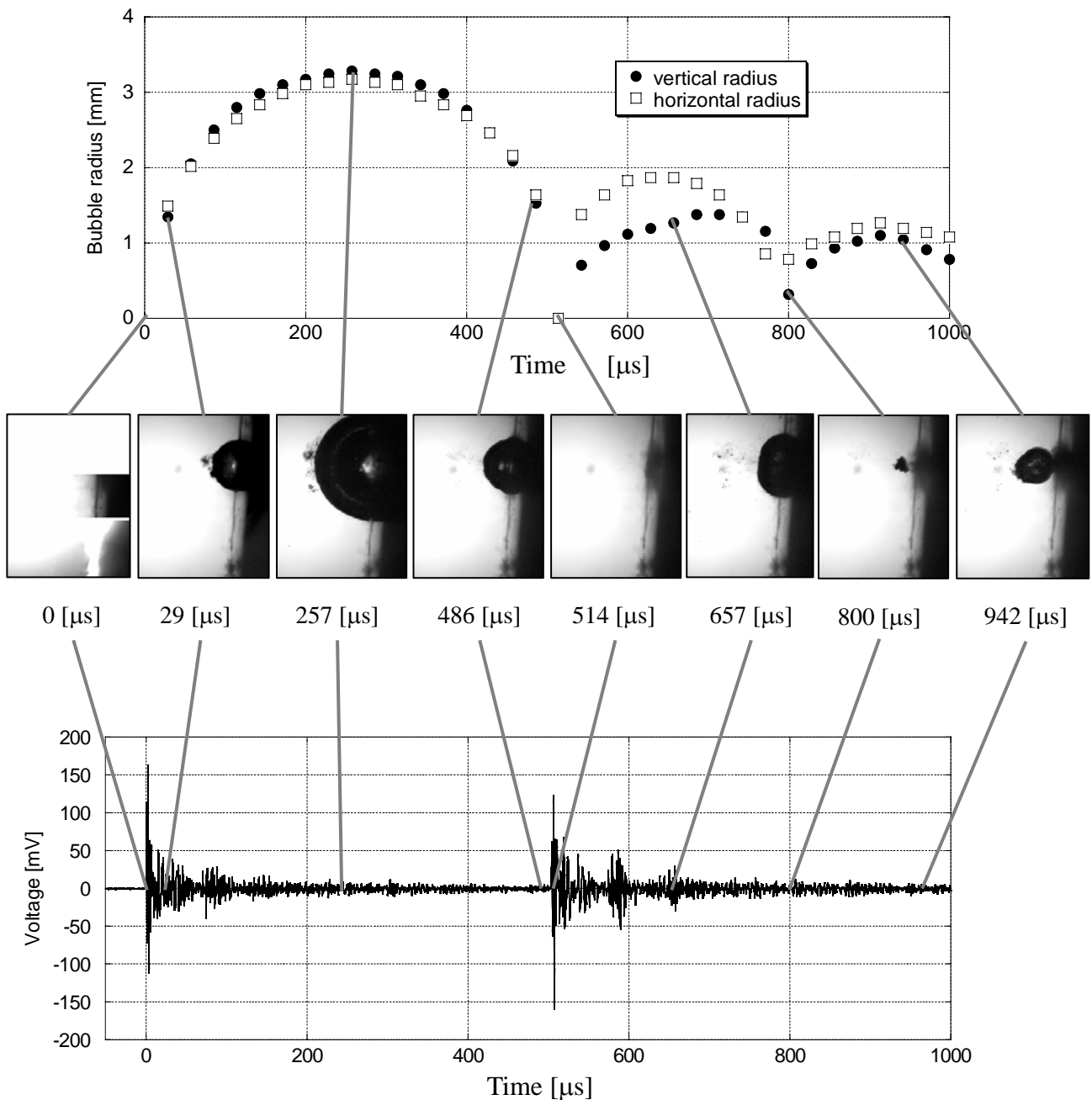


Figure 3. Transition of bubble radius and detected AE waveform in set-up (a)-2 (laser energy: 100mJ, water temperature: 25.1°C)

3. Results and discussion

3.1 Detected AE waveform compared with photos by high speed camera

During laser shock peening process, a bubble was generated after laser irradiation. Fig. 3 shows typical AE waveforms detected during laser peening process coupling with photos recorded by the high speed camera and a graph demonstrated a change of radius of a bubble on sample surface. Two AE events were generated with time duration of several hundred microseconds for each laser irradiation. The results of high speed camera showed that after laser irradiation a bubble generated and expanded its size up to the maximum radius. Then it became smaller and finally collapsed. According to this observation, the first and latter AE events were considered to correspond to laser irradiation and bubble collapse, respectively. Let t_1 and t_2 are times for the first and second AE events, respectively while t_c and R_{max} are time for bubble collapse and maximum bubble radius obtained from the high speed camera results, respectively. A time interval between two events, Δt , is defined as $t_2 - t_1$. A plot of Δt vs. t_c and R_{max} vs. t_c for experiment condition (a)-1 is shown in Fig. 3 and 4, respectively. A linear relationship of these parameters supported that the first and latter AE events were generated from impacts due to laser irradiation and bubble collapse, respectively. Fig. 4 shows a plot of in room temperature. It is clear that larger bubble required longer collapse time at constant temperature.

3.2 A cavitation bubble

A cavitation bubble was generated by laser irradiation, expanded, shrank and collapsed. A bubble was almost hemisphere, but after bubble collapse a bubble became ellipsoid, repeated expanding and shrinking, and finally became some smaller bubbles (Fig. 3). In the case of laser irradiation from horizontal direction (Fig. 1(a)), a bubble comes off the sample after second collapse, so AE event was not detected. In case of laser irradiation from vertical direction (Fig. 1(b)), they are sometimes detected more AE event than three when a bubble does not come off. Time detected third and fourth AE event is equal to second and third bubble collapse time respectively (Fig. 5).

By using HyperVision HPV-2A, collapse of a cavitation bubble was observed in detail with the sampling rate of 1,000,000 fps and pixels of 312×256 (Fig. 6). Immediately after bubble collapse,

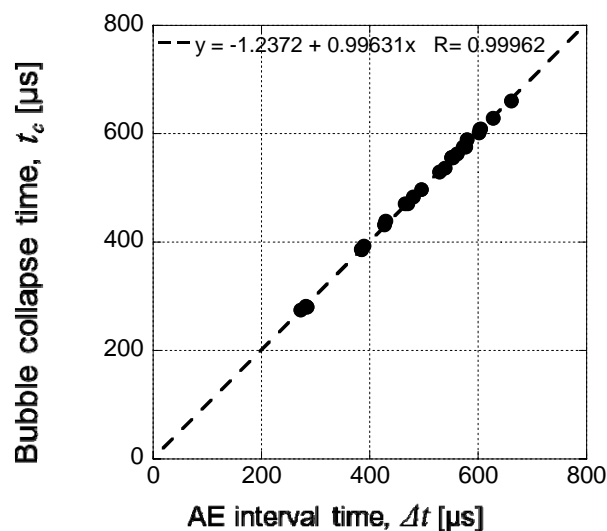


Figure 4. Relationship between bubble collapse time, t_c and AE interval time, Δt in room temperature

it was emitted a hemisphere tremor from the center of a bubble before collapse. The speed of propagation of the tremor is about 1,500 m/s, so the tremor was caused by shock wave due to bubble collapse.

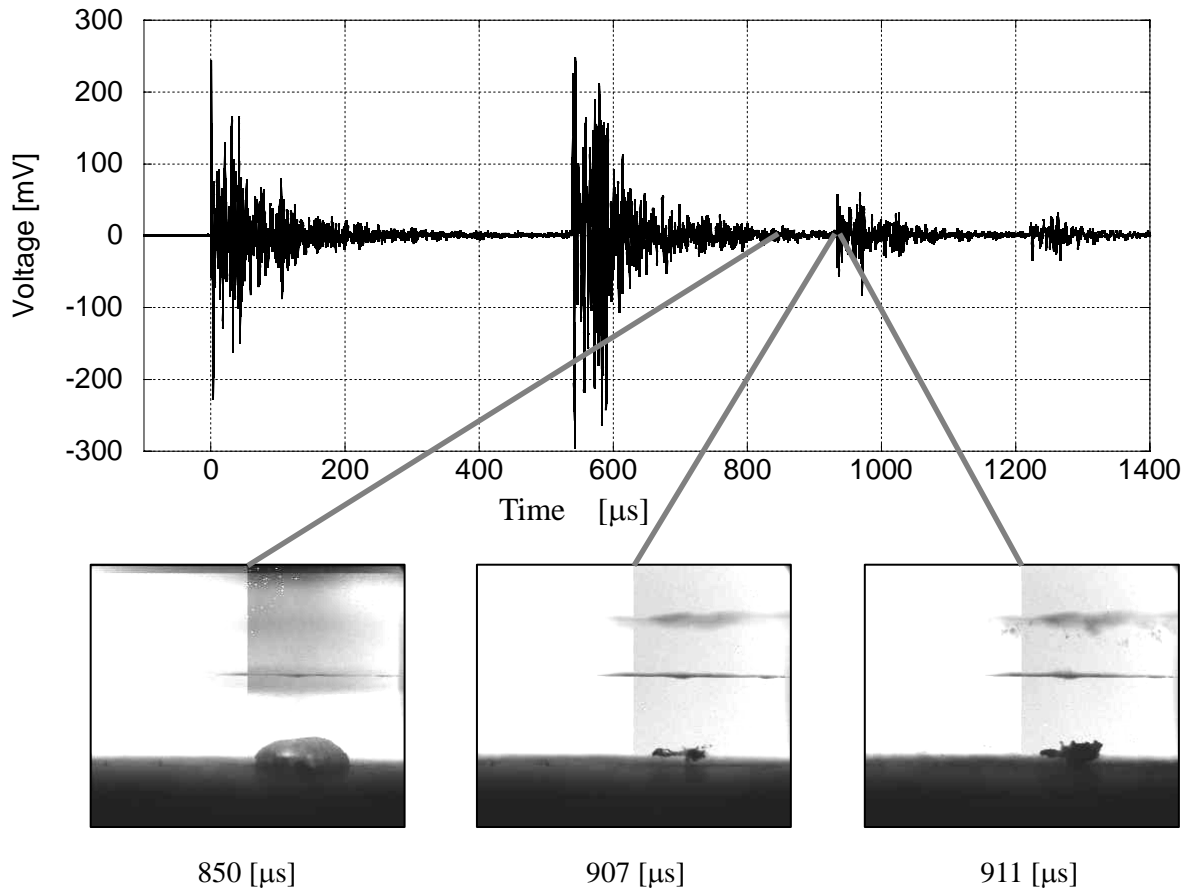


Figure 5. Detected AE waveform in set-up (b), (laser energy: 100mJ, water thickness: 5mm)

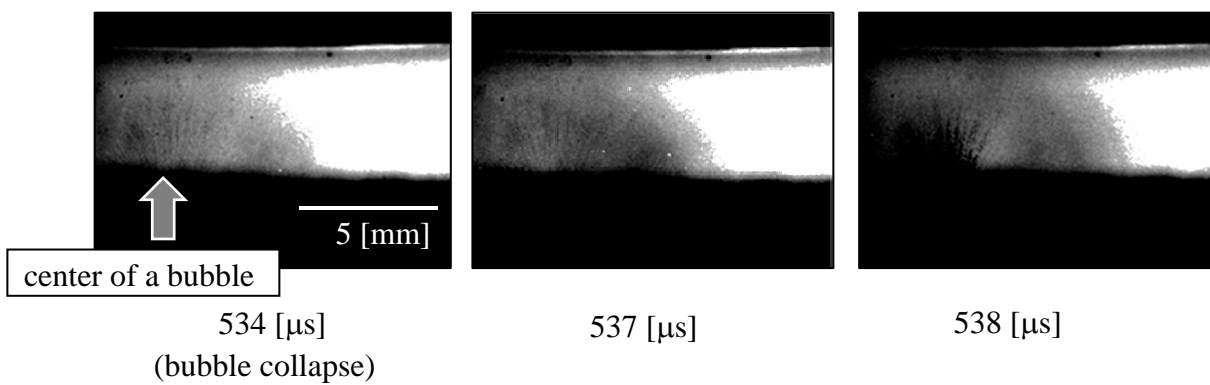


Figure 6. Optical observation of propagation of shock wave by bubble

3.3 Effect of water temperature

In Fig. 7, maximum radius of a cavitation bubble, R_{max} is plotted with AE interval time, Δt . A relationship between maximum radius of a cavitation bubble and bubble collapse time is linear in room temperature. On the other hand, the relationship in experiment with varying water temperature is not linear as shown in Fig. 8. In Fig.9, maximum bubble radius, R_{max} is plotted for water temperature, T_w . The maximum radius of a cavitation bubble increases with water temperature. These results suggested that temperature affects the maximum radius and shape of a bubble.

The graph in Fig. 10 shows a plot of impact forces of laser irradiation, I_L and these of bubble collapse, I_B with water temperature. Impact force from laser ablation became smaller than that from laser irradiation with increasing water temperature. Fig. 11 shows a plot of a ratio of impact forces due to laser irradiation and bubble collapse, I_B / I_F with water temperature. Impact forces from laser irradiation are not affected by water temperature. On the other hand, impact force from bubble collapse became smaller than that from laser irradiation with increasing water temperature and the ratio of I_B / I_F decrease clearly in Fig. 11.

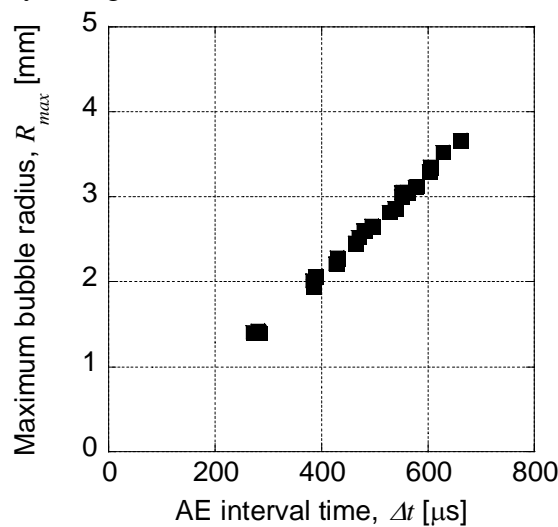


Figure 7. Relationship between maximum bubble radius, R_{max} and AE interval time, Δt in room temperature

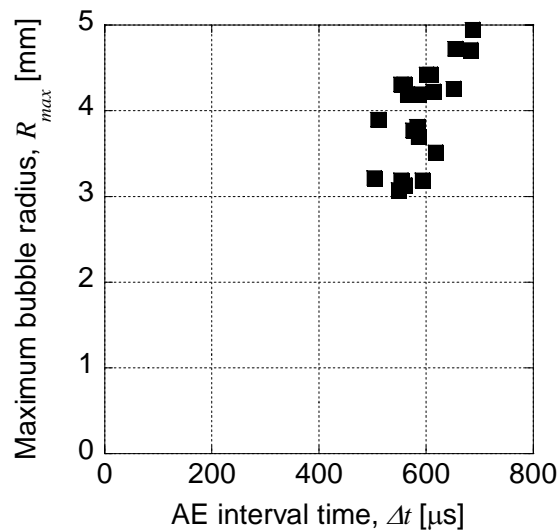


Figure 8. Relationship between maximum bubble radius, R_{max} and AE interval time, Δt with varying water temperature

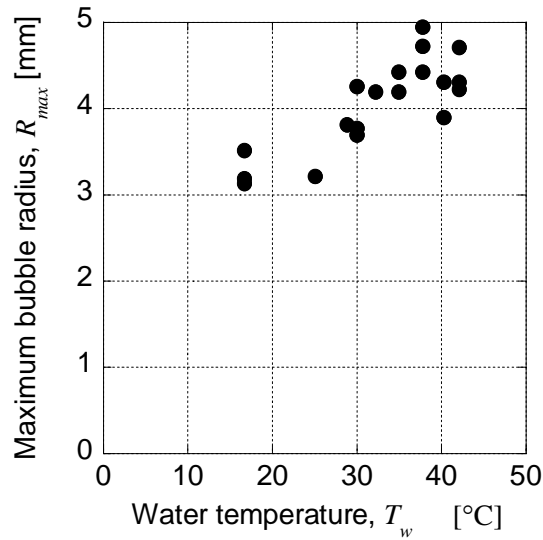


Figure 9. Relationship between water temperature, T_w and AE event interval, Δt

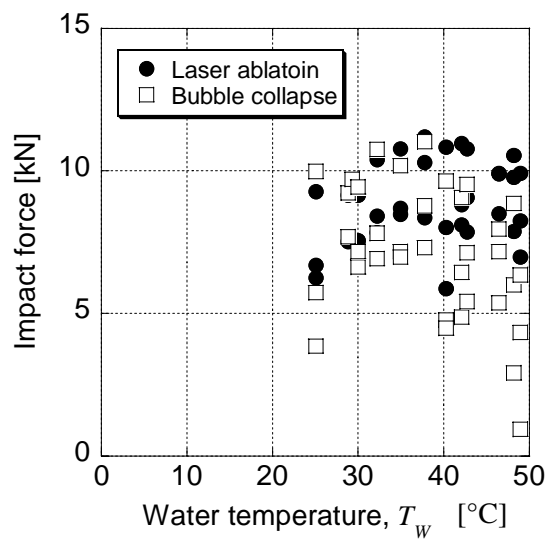


Figure 10. Relationship between water temperature, T_w and impact force, I_L and I_B

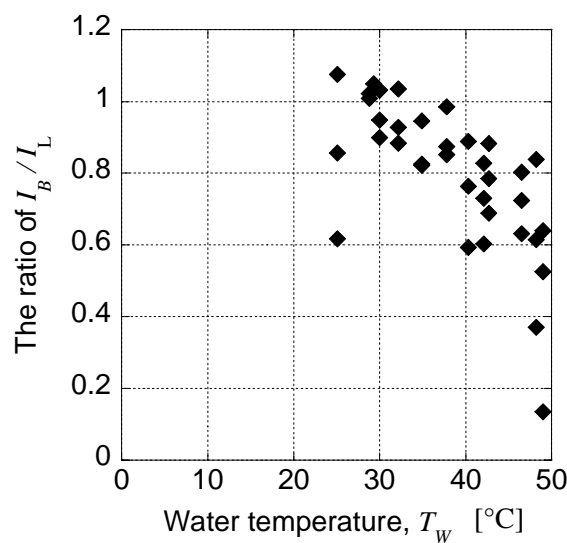


Figure 11. Relationship between water temperature, T_w and the ratio of I_B / I_L

3.4 Effect of thickness of water layer

In experimental set-up (b), impact forces during laser shock peening process were obtained from detected AE waveforms by deconvolution technique, which is plotted in Fig. 12 as a function of water layer thickness. When the water layer was thinner than 2 mm, impact forces of laser irradiation and a bubble collapse were very small. Impact force by a bubble collapse showed the maximum value when thickness of water layer was 3-5 mm, while impact force by laser irradiation was a certain value.

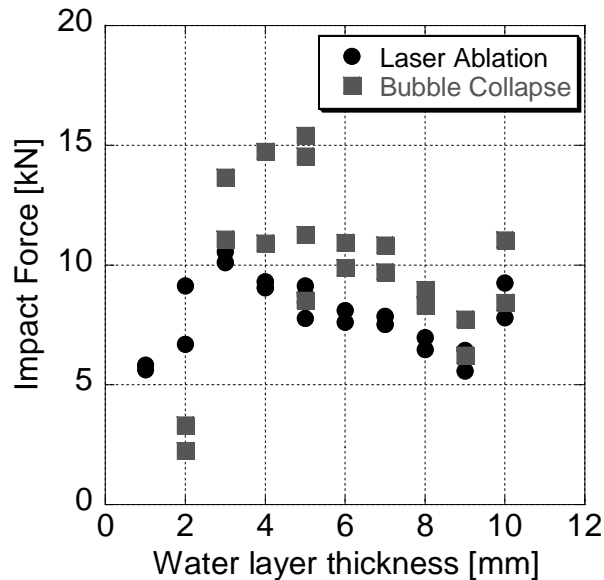


Figure 12. Relationship between water layer thickness and impact

4. Conclusions

In the present study, the effect of water layer and temperature in laser shock peening was evaluated by AE method and high speed camera, and following conclusions were drawn;

- (1) Impacts were emitted by not only laser irradiation but also bubble collapsed.
- (2) Maximum radius of a cavitation bubble increases with temperature of water layer and has a linear relationship with AE event interval time in constant temperature.
- (3) Impact forces of laser irradiation are not affected by water temperature. Impact forces of bubble collapse decrease with increasing water temperature. The ratio of two impact forces due to laser ablation and bubble collapse decreases with increasing water temperature.
- (4) Impact forces by laser irradiation and bubble collapse have the maximum value at the of water layer thickness around 4 mm.

Acknowledgement

This work was partially supported by JSPS KAKENHI Grant Number 23246124.

References

- [1] D.J. Buttle, C.B. Scruby, Characterization of particle impact by quantitative acoustic emission, *Wear*, 137(1990) 63-90
- [2] M. Enoki, K. Kobayashi, T. Tomoki, M. Matsui, Y. Kobayashi, Quantitative Acoustic Emission Measurement of Laser Peening in EWGAE 2012
- [3] K. Ito, M. Enoki, Acquisition and Analysis of Continuous Acoustic Emission Waveform for Classification of Damage Sources in Ceramic Fiber Mat, *Mater. Trans.*, 48 (2007) 1221-1226.